G. Basic Studies of Ultrasonic Welding for Advanced Transportation Systems

Principal Investigator: Zhili Feng
Oak Ridge National Laboratory
1 Bethel Valley Road, Oak Ridge, Tennessee 37831
(865) 576-3797, (865) 574-4928, e-mail: fengz@ornl.gov

Technology Development Area Specialist: Sidney Diamond
(202) 586-8032; fax: (202) 586-1600; e-mail: sid.diamond@ee.doe.gov
Field Technical Manager: Philip S. Sklad
(865) 574-5069; fax: (865) 576-4963; e-mail: skladps@ornl.gov

Contractor: Oak Ridge National Laboratory
Contract No.: DE-AC05-00OR22725

Objective

- Develop a fundamental understanding of the ultrasonic welding (UW) process.
- Establish process conditions to optimize joint properties of aluminum (Al) alloys for auto body applications.
- Explore opportunities for joining dissimilar materials.
- Explore the feasibility of ultrasonic processing in other novel and unique situations in materials processing such as making powders more dense, producing functionally graded components, modifying surface properties, and producing dissimilar material joints.

Approach

- Perform UW experiments to develop correlations of process parameters with joint properties.
- Characterize details of joint microstructures.
- Model the fundamental interactions of ultrasonic waves with solids.

Accomplishments

- Purchased and installed the UW system.
- Demonstrated the breadth of potential applications of the UW process, namely, the feasibility of metallurgical bonding of steel, Al, and magnesium (Mg) alloys to themselves and bonding of dissimilar joints between steels and Al alloys.
- Observed certain unique phenomena at the bonding interfaces under different process conditions,
- Initiated development of theoretical models to determine the vibration amplitude distribution in simple plate configuration.

Future Direction

- Continue the welding process development for dissimilar materials, including joining amorphous metals.
- Study the structure-property relationship of joints.

- Conduct experiments to determine the importance of vibration normal to the bond interface in the bonding process.
- Model the acoustic energy distribution in the weld joint.
- Study the residual stress distribution in the bonding region.
- Assess the ability of ultrasonic processing to enhance the densification of powder metal compacts.
- Explore the feasibility of ultrasonic bonding of nanoparticles.

Introduction

In response to a highly competitive global market, environmental concerns, and the government fuel conservation and safety mandates, the U.S. automotive industry is aggressively pursuing high-performance and energy-efficient vehicles that involve increased use of lightweight and high-strength materials (such as Al alloys, composites, Mg alloys, and advanced high-strength steels). The use of these new materials presents significant technical challenges to the existing body-assembly joining processes such as electrical resistance spot welding (RSW). A number of issues exist in applying RSW to Al sheet metals and coated steels, including unacceptable electrode life, weld quality, and performance. Furthermore, because of metallurgical incompatibility, fusion welding of dissimilar metals (Al to steel, for example) is generally very difficult, if not impossible.

As material joining is one of the major manufacturing processes used to assemble auto-body structures, the auto industry is actively considering a number of alternative welding technologies that would enable the increased use of lightweight and high-performance materials. Many of the alternative processes involve innovative solid-state joining in which metallurgical bonding between the same or dissimilar materials can be created without melting. One of the solid-state-based joining processes is UW.

UW relies on mechanical vibrations at frequencies higher than the upper limit of normal human hearing (about 18 kH). Figure **1** shows the basic process setup for making spot welds in metals. An electromechanical converter (such as a piezoelectric transducer) converts high-frequency electric current to mechanical vibrations. The mechanical vibration is then modulated and amplified by the booster/horn before it is applied to the workpiece through the sonotrode. A moderate clamping force is applied to ensure the mechanical vibration is transferred to the sheet-to-sheet interface (the faying surface) where the weld is created. Typically, the mechanical vibration is at 20–40 kHz with an amplitude range of 5 to 50 μm. The power delivered to the workpiece is in the range of several hundred to several thousand watts, although more powerful UW power sources are being developed. Another important aspect that must be considered in auto-body assembly is the production rate. The welding time of UW is relative short, usually in the range of a less than a second to several seconds. This is in principle comparable to the production rate of electric RSW currently used in assembly lines.

As far as the basic bonding process is concerned, UW is a variation of friction welding. As shown in Figure 2, the combination of clamp pressure and mechanical vibration produces several important effects in the formation of the metallurgical bond at the workpiece interface. The lateral mechanical vibration of the sonotrode causes a small amount of relative motion between the workpieces at

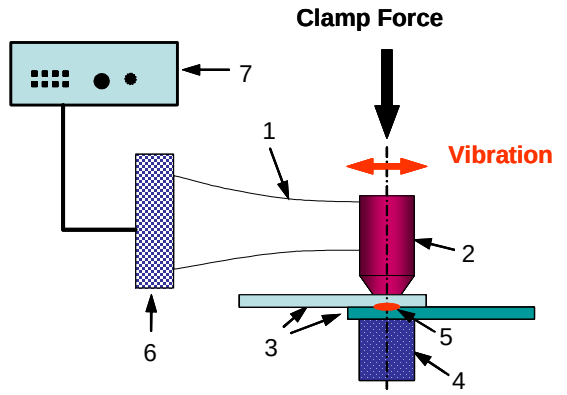

1 – Welding Horn 2 – Sonotrode
3 – Workpiece 4 – Anvil
5 – Weld 6 – Piezoelectric transducer
7 – High freq electric current generator

Figure 1. Schematic setup of ultrasonic welding process.

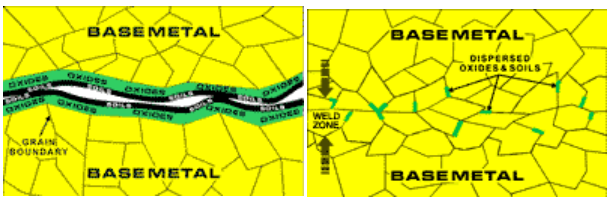

Figure 2. Schematic representation of bond interface before (left) and after (right) ultrasonic welding.

the interface. The frictional action at the interface due to the relative motion and the pressure breaks the surface oxides and other contaminants. As a result, clean metal surfaces are brought into contact under pressure. Frictional heating also occurs at the bond interface. The heating promotes both localized deformation and diffusion in the region where the pressure is applied. Similar to other friction welding processes, when this process is optimized, metallurgical bonds can be obtained without melting at the bonding interface. The self-cleaning nature of UW and its ability to form metallurgical bonds without melting are both important advantages of the process. Another characteristic of UW that could be exploited is its apparent ability to soften metals as a result of the interactions of ultrasonic waves with microstructural features. This phenomenon is known as acoustic softening.

UW creates a joint without bulk melting. Thus, the ultrasonic weld is inherently immune to welding defects associated with the solidification process in fusion welding. These include the solidification cracking and porosity due to absorption of gaseous impurities (N, H, O) by the liquid metal that are common in electrical RSW of Al alloys. Also, unlike the copper-based electrode used in electrical RSW, the sonotrode in UW can be made of high-strength materials that are inert to chemical attaching from the material to be welded. It is expected that the life of the sonotrode would not be a critical factor limiting the production rate and the quality of the welds. Therefore, UW offers several significant advantages over current methods of joining Al alloys. Indeed, industry test data indicate that compared with resistance spot welded Al, ultrasonic joints have higher and more predictable strength and weld quality. The UW process is considered to be one of the primary candidates for spot welding of Al body structures.

At present, studies by the auto industry have been primarily on nonheat treatable 5××× series Al alloys, focusing on application issues. This program investigates UW of heat-treatable and other lightweight materials, including the joining of dissimilar materials such as steel to Al and Al to Mg.

Welding

Welding trials were conducted on a Sonobond UW system, acquired specifically for this program. The machine operated at 20 kHz and had a maximum rated power output of 2500 W. The welding system, shown in Figure 3, consists of a power supply and the welder. The power supply generates 20 kHz of electric current, which is fed to the piezoelectric transducer in the welder. The mechanical ultrasonic vibration is transferred to the workpiece through the horizontal mounted horn and the vertical

Figure 3. The Sonobond ultrasonic welder used in this program.

sonotrode. The clamping pressure was applied pneumatically by compressed air.

All welds were made using a 1 × 4-in. coupon as shown in Figure 4. This is a standard coupon dimension commonly used by the auto industry for weldability testing of resistance spot welds.

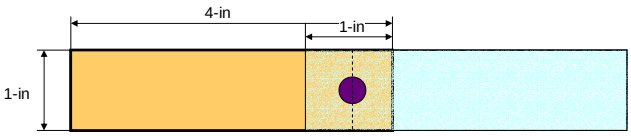

Figure 4. Coupon dimension used in welding trials.

The feasibility of UW of various combinations of materials (Al alloys, steels, Mg alloys) commonly used in the automotive industry was investigated first. Most materials tested had a nominal thickness of 1 mm. It was found that the UW process was relatively robust. The following material combinations were successfully bonded together in this program (see Figure 5):

- Al1100 to Al1100
- Al3003 to Al3003
- Al2024 to Al2024
- Al6061 to Al6061
- Al6111 to Al6111
- Al6061 to Al2024

Figure 5. Ultrasonic welds made of various material combinations. From top to bottom: Al2024 to Al6111, Al6111 to Al6111, Al2024 to Al2024, Al1100 to Al1100, DQSK steel to Al2024, DQSK steel to DQSK steel, and Mg AZ31 to Mg AZ31.

- Al6111 to Al2024
- DQSK steel to DQSK steel
- DQSK steel to Al2024
- Mg alloy AZ31 to Mg alloy AZ31

It should be noted that, although metallurgical bonding of these material combinations was feasible, the mechanical properties of some of the material

combinations need to be improved through welding process development and optimization that are planned in FY 2004.

In an effort to investigate the interface phenomena during UW, a series of dissimilar welds between Al2024-T3 and Al6061-T4 were made under various energy and clamping force conditions. These two Al alloys have very different etching response rates to Keller's reagent. This allowed for selective etching to reveal the interface region of the weld. This approach circumvented the difficulties in studying the bonding interface made of the same material.

The baseline conditions for a good-quality weld were at 750 J and 70 psi. A process range test revealed that, under the current testing setup, no metallurgical bonding was produced when the energy level was below 500 J. When the energy input exceeded 1000 J, severe sticking of the workpiece to either the sonotrode or the anvil was experienced. Thus, the following process parameter ranges were selected for the bonding interface study:

- Power: 2400 W
- Energy range: 500 to 1000 J in 50 J increments
- Pressure: 50 to 90 psi in 10 psi increments

It should be noted that the impedance of the system could vary significantly during welding. Thus, the actual welding power level is not a constant but varies accordingly during the process. The actual welding power variations during welding were not measured in this phase of the program.

Microstructure Characterization

Both optical microscopy (OM) and scanning electron microscopy (SEM) were employed to characterize the microstructure changes in the vicinity of ultrasonic welds. The initial portion of this study concentrated on ultrasonic welds between dissimilar Al alloys (Al2024 and Al6061). The difference in etching rates of the two alloys in Keller's reagent was used to distinguish the two alloys, especially at the weld interface (see Figure 6). In a similar fashion, the difference in average atomic numbers between the alloys permitted backscattered electron (BSE) imaging to reveal the distribution of the different alloy regions as well as precipitate phases (Figure 7).

The macrostructure of two 2024/6061 ultrasonic welds is compared in Figure 6. The two welds were produced at the same power setting (2400 W) but at different ultrasonic energy levels (750 and 950 J). In all the microstructure photos in this section, the Al2024 was the upper sheet and was in direct contact with the vibrating sonotrode, which applied both the ultrasonic energy and the bonding pressure. The Al6061 was the lower sheet and was supported by the stationary anvil. From Figure 6(a), the weld interface appears as a good metallurgical bond over a diameter slightly wider than the impression left by the sonotrode (indicated by the roughening of the upper surface of the Al2024 sheet by the knurled surface of the sonotrode). A significant bowing of the weld interface occurs into the Al6061 sheet near the center of the weld relative to the unjoined surfaces. As the lower surface of the Al6061 sheet is essentially flat, it appears that mass transport of the Al6061 has occurred. A similar bowing of the weld interface into the Al6061 plate occurred for the higher-power weld (Figure 6b), though the effect is less obvious as a result of the slight bending of the entire welded piece that might result from the welded piece sticking to the anvil at this high energy level and subsequent straining of the specimen during removal. A slight waviness of the weld interface occurs at the higher ultrasonic power level.

Both OM and SEM examination of the edges of the ultrasonic weld at higher magnification revealed structures that indicated extensive material deformation at the interface. The surface appeared to

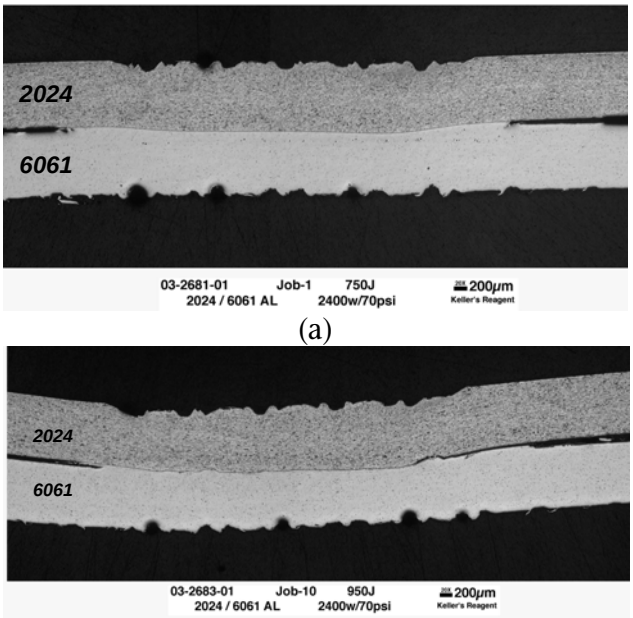

Figure 6. Optical micrographs of Al2024 and Al6061 ultrasonic welds made at 2400 W and 70 psi: (a) 750 J and (b) 950 J.

undergo extensive folding/extrusion due to the friction action at the interface. This effect was more pronounced at higher bonding pressure (90 psi in Figure 7). The OM (Figure 7a) of the etched weld reveals flow lines in the deformed material, and BSE images of the same area in the SEM (Figure 7) Images show that the extruded material is all the darker-imaging Al6061. In addition to the deformation, most of the weld edges exhibit cracklike features, which are always into the Al6061 side of the interface, never into the Al2024. The causes for the formation of this type of feature are not clear at the moment, and further studies are planned to understand this phenomenon. The undeformed base Al6061 material exhibits fine (5–50 μm) original grain structure, as shown in Figure 7b. However, the grain structure of the deformed material at the interface is not apparent even at higher magnification or BSE contrast level. It is presumed that the high residual stress and dislocation density in the extruded material significantly reduce the BSE channeling contrast responsible for the grain structure

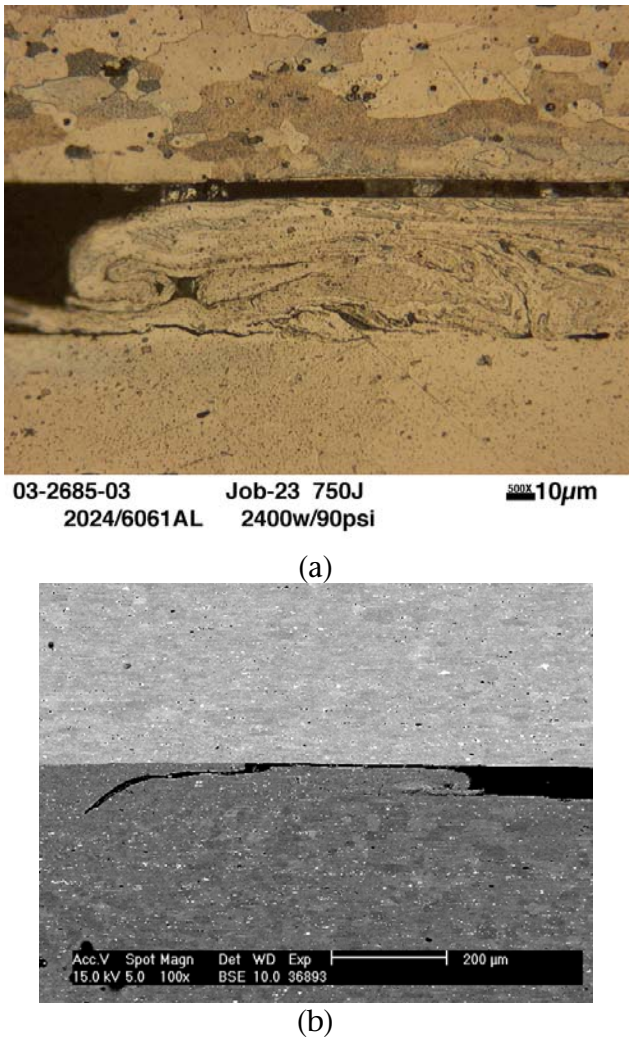

Figure 7. (a) Optical micrograph and (b) SEM micrographs of Al2024/Al6061 ultrasonic welds made at 2400 W ultrasonic energy, 750J power, and 90 psi. The Al2024 material is the upper sheet.

contrast in the relatively undeformed Al6061 base matrix.

The BSE images reveal other microstructural features of the ultrasonic welds at higher magnification, including the weld interface structure and the precipitate structure. The increased tendency for waviness of the weld interface with increased ultrasonic energy input is shown in Figure 8. At 750 J power, the interface is generally flat to within 1–2 μm (Figure 8a), whereas waviness of ~10–20 μm is observed

at 950 J (Figure 8b). The difference in the BSE image contrast of the two alloys permitted the extent of intermixing during UW to be estimated (Figure 9a). At some regions of the weld interface, the BSE contrast changes between those two levels over distances of ~300 nm. This is an upper estimate for the zone of intermixing at the interface because the spatial resolution of BSE images is determined by both the incident probe (nominally <10 nm) and the lateral extent of the excited volume for BSE emission at 5 kV (~250 nm). Therefore, the observed resolution of the BSE image at the weld interface is dominated by the excited volume and does not represent the actual width of the transition zone.

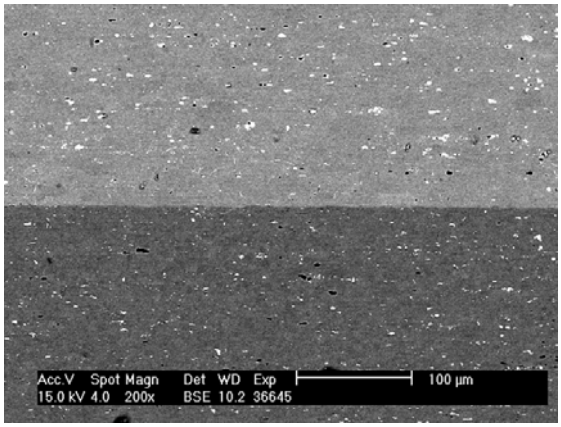

(a)

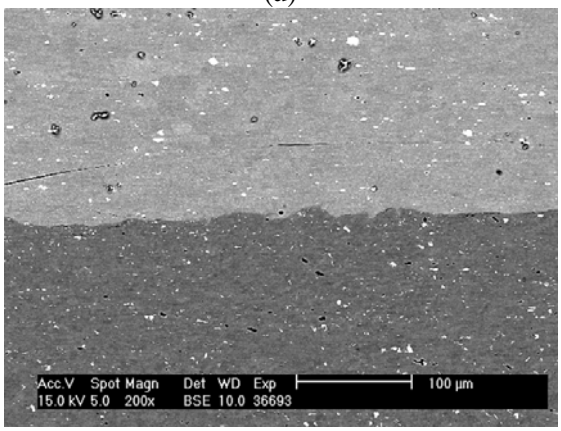

(b)

Figure 8. BSE images of 2024Al/6061Al ultrasonic welds made at 2400 W, 70 psi and either (a) 750 or 950 J power. The 2024Al material is the upper sheet.

The precipitate microstructure of both alloys is revealed in Figure 9b.

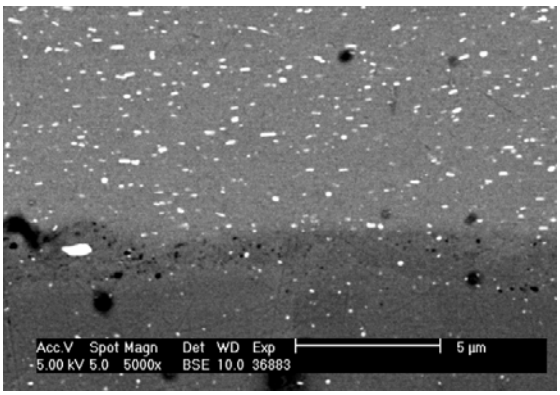

(a)

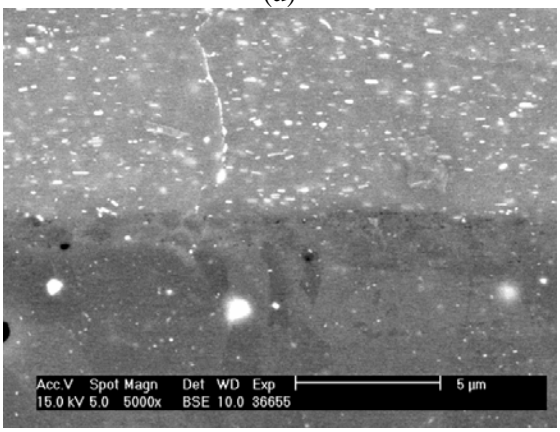

(b)

Figure 9. BSE images of Al2024/Al6061 ultrasonic welds (2400 W, 750 J and 70 psi). Al2024 is the upper sheet. The bright line in (b) is presumed to be dislocation decorated by Cu-enriched precipitates.

The coarse precipitates in the Al6061 are enriched in Fe and Si with lower enrichment of Cr and Mn relative to the matrix, whereas the precipitates in the Al2024 are Cu-enriched. The bright line in the Al2024 matrix is taken as evidence of heterogeneous nucleation of Cu-enriched precipitates on a dislocation. No evidence exists of a gradient in either size or number density of the Cu-enriched precipitates as a function of distance from the weld interface. In addition, the observed precipitate microstructure near the weld interface is

comparable to that observed in the unbonded Al2024 sheet more than 5 mm outside of the weld. This observation indicates that the local heating near the weld interface from the localized absorption of ultrasonic energy does not exceed the solvus temperature for the Cu-enriched precipitates. If this phase is the equilibrium θ phase, the maximum temperature must be <490°C and therefore below both the melting temperature of Al and the eutectic temperature of the alloy. If the precipitate phase were one of the metastable phases, the maximum temperature would be lower, as the solvus of these precipitates is lower than that of the equilibrium phase. For these reasons, the mechanism of UW does not involve melting, even localized melting at the interface.

In some of the BSE images near the weld interface, there are indications of a narrow zone at the interface that exhibit slightly different contrast (e.g., 1–2 μm in thickness in Figure 10a). As this dimension is significantly smaller than the average grain sizes of either alloy near the weld interface (~10 μm for the Al6061 and ~30 μm for the Al2024), electron backscatter diffraction (EBSD) and orientation imaging microscopy in the SEM were used to further characterize the microstructure near the weld interface. Image quality maps reflect the clarity of the EBSD pattern at each point in the map and reveal the local microstructure (Figure 10a). The coarser grain structure of the Al2024 is evident, and a narrow, dark band is present at the weld interface. This lower image quality probably indicates localized strain in that region. Smaller grains are present in the Al2024 adjacent to the dark interface zone. These grains may indicate recrystallization of a layer of deformed material. Inverse pole figure maps reflect the local crystallographic orientation of a specified direction (e.g., surface normal) at each point in the map (Figure 10b). The shades of the local orientation reveals that the dark layer at the

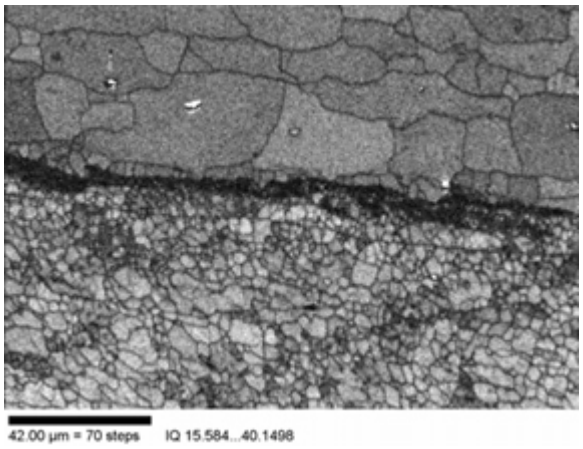

(a)

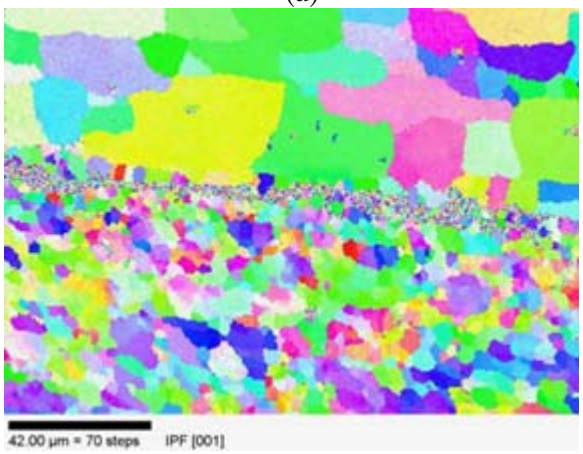

(b)

Figure 10. Orientation imaging maps for Al2024/Al6061 ultrasonic weld made at 2400 W ultrasonic energy, 750 J power and 90 psi. Shade/color coding in (b) gives the crystallographic orientation of the local surface as normal. The Al2024 is the upper sheet.

interface does not exhibit a grain structure at the resolution of this inverse pole figure map (~1 μm). In related work with Ford Research and Advanced Engineering under a recent MPLUS project, we were able to demonstrate that both recovered and recrystallized regions were at the weld interfaces of ultrasonically welded 6111Al. That work required inverse pole figure maps at spatial resolutions of 0.2 μm. In order to acquire such maps for the current materials, the development of an improved specimen-

preparation technique for these dissimilar alloy welds will be required.

Process Modeling

In order to determine the displacement amplitude distribution generated in a plate during UW, two different numerical techniques were used to solve the wave equation for a plate. The first technique was a decomposition of the problem by setting up dual grids for the in-plane x- and y-displacements. These quantities satisfy two coupled second-order partial differential equations derived from elastic plate theory. By treating the problem in this manner, we can solve the resulting homogeneous matrix equations by singular-value decomposition methods, which is much faster than comparable finite-element and finite-difference methods. Boundary conditions on the plate (i.e., clamped edges, where the displacements are zero, or free edges, where the stresses are zero) can be varied to suit the application simply by changing the appropriate elements of the decomposition matrix; thus this approach is well-suited to modification that will permit driving the plate with an external source, as occurs during UW.

The second technique is a new PDE solver that converts the problem into a simple boundary element problem. This approach solves the wave equation analytically for any set of boundary points, thus allowing much higher precision of the solution without requiring more computer memory and time.

Computer codes were developed, implementing both techniques to find the eigen values (resonance frequencies) and eigen vectors (displacements) for a rectangular plate. The first example tested was to solve for the in-plane (extensional) resonant modes for a square plate one unit on a side, having clamped edges. Our programs found a series of such resonances, the first occurring for a normalized frequency of 0.578. Assuming Al for the plate material and a size of one meter square, this corresponds to a frequency of about 3.1 kHz; thus for the plate sizes of interest to this program, the driving point of the ultrasonic transducer will probably be quite critical. This value would scale inversely with the plate dimension. The program also determines the plate displacements for each mode, which can then be plotted. Examination of the first few modes yielded displacement patterns typical of elastic resonant modes and provided confidence that the code is working correctly.

Knowing the resonant frequency and modes is important for the study of UW. First, from our results it is evident that small plates should behave differently from large plates at the same frequency. This point has not been considered before in the study. Second, the type of resonance oscillation will impact the distribution of acoustic energy, thus influencing the efficiency of the welding process. More detailed study is needed for understanding the dependence of the energy distribution on the size and the shape of the plates.

Conclusions

A number of major accomplishments and significant progress have been made in FY 2003. The program progressed well along the proposed milestones. Feasibility has been demonstrated for UW of steel and Al and Mg alloys to themselves, and for welding dissimilar joints between steels and Al alloys. The interface study using dissimilar welds between Al2024 and Al6061 revealed a number of important phenomena at the interface under different process conditions. The development of theoretical models allows for interrogation of the geometry effects on the distribution of acoustic energy that would have significant implications in the application of the UW process.

Acknowledgements

Dr. Michael Santella, Dr. Edward A. Kenik, Dr. Xiaoguang Zhang, and Dr. William Simpson of Oak Ridge National Laboratory were part of the program team. Their contributions to the program are acknowledged.